

# Redistribution at silicon by ruthenium complexes. Bonding mode of the bridging silanes in $\text{Ru}_2\text{H}_4(\mu\text{-}\eta^2\text{:}\eta^2\text{:}\eta^2\text{-SiH}_4)(\text{PCy}_3)_4$ and $\text{Ru}_2\text{H}_2(\mu\text{-}\eta^2\text{:}\eta^2\text{-H}_2\text{Si}(\text{OMe})_2)_3(\text{PCy}_3)_2$ †

Ridha Ben Said,<sup>‡a</sup> Khansaa Hussein,<sup>§a</sup> Jean-Claude Barthelat,<sup>a</sup> Isabelle Atheaux,<sup>b</sup> Sylviane Sabo-Etienne,<sup>\*b</sup> Mary Grellier,<sup>b</sup> Bruno Donnadieu<sup>b</sup> and Bruno Chaudret<sup>b</sup>

<sup>a</sup> Laboratoire de Physique Quantique, IRSAMC (UMR 5626), Université Paul Sabatier, 118 route de Narbonne, 31062 Toulouse Cedex 4, France

<sup>b</sup> Laboratoire de Chimie de Coordination du CNRS, 205 route de Narbonne, 31077 Toulouse Cedex 04, France. E-mail: sabo@lcc-toulouse.fr; Fax: +33 5 61 55 30 03; Tel: +33 5 61 33 31 77

Received 14th April 2003, Accepted 15th July 2003

First published as an Advance Article on the web 22nd September 2003

The bis(dihydrogen) complex  $\text{RuH}_2(\eta^2\text{-H}_2)_2(\text{PCy}_3)_2$  (**1**) reacts with 2 equiv. of  $\text{H}_2\text{SiMePh}$  to produce a mixture of  $\text{Ru}_2\text{H}_4(\mu\text{-}\eta^2\text{:}\eta^2\text{:}\eta^2\text{-SiH}_4)(\text{PCy}_3)_4$  (**2**) and  $\text{RuH}_2(\eta^2\text{-H}_2)(\eta^2\text{-HSiPh}_3)(\text{PCy}_3)_2$  (**4**) together with  $\text{HSiMePh}_2$ ,  $\text{HSiMe}_2\text{Ph}$  and traces of  $\text{HMe}_2\text{SiSiMe}_2\text{H}$  as a result of redistribution at silicon. The bridging  $\text{SiH}_4$  ligand in **2** is coordinated to the two ruthenium *via* four  $\sigma\text{-Si-H}$  bonds in agreement with NMR, X-ray data (on **2**, and **2'** the analogous  $\text{P}^i\text{Pr}_3$  complex) and DFT calculations. Each interaction involves  $\sigma$ -donation to a ruthenium and back-bonding from the other ruthenium. Elimination of  $\text{SiH}_4$  and formation of  $\text{RuH}_2(\text{CO})_2(\text{PCy}_3)_2$  (**5**),  $\text{RuH}_2(\text{tBuNC})_2(\text{PCy}_3)_2$  (**6**) or  $\text{RuH}(\eta^2\text{-H}_2)\text{Cl}(\text{PCy}_3)_2$  (**7**) were observed upon the reaction of **2** with  $\text{CO}$ ,  $\text{tBuNC}$ ,  $\text{CH}_2\text{Cl}_2$ , respectively. No reaction occurred in the presence of  $\text{H}_2$ , but H/D exchange was observed under  $\text{D}_2$  atmosphere. Another redistribution reaction at silicon can be obtained by adding 4 equiv. of  $\text{HSi}(\text{OMe})_3$  to **2** to produce  $\text{Si}(\text{OMe})_4$  and  $\text{Ru}_2\text{H}_2(\mu\text{-}\eta^2\text{:}\eta^2\text{-H}_2\text{Si}(\text{OMe})_2)_3(\text{PCy}_3)_2$  (**3**) displaying three bridging ( $\mu\text{-}\eta^2\text{:}\eta^2$  alkoxy silane) ligands. Complex **3** is characterized by multinuclear NMR spectroscopies and by a crystal structure. DFT calculations show that the model complex  $\text{Ru}_2\text{H}_2(\mu\text{-}\eta^2\text{:}\eta^2\text{-H}_2\text{Si}(\text{OR})_2)_3(\text{PR}_3)_2$  ( $\text{R} = \text{H}, \text{Me}$ ) is a minimum on the potential energy surface, and support the dihydride formulation with three bridging  $\text{H}_2\text{Si}(\text{OMe})_2$  ligands coordinated to the two ruthenium through  $\sigma\text{-Si-H}$  bonds.

## Introduction

Redistribution represents an important reaction in silane chemistry. This process is normally catalyzed by strong bases and strong acids, whereas catalysis by transition metal complexes has not been very much developed.<sup>1</sup> However, in this latter case, the reactions could be more specific leading to useful applications. In this context, the possibility to generate the simplest silane  $\text{SiH}_4$  can be an interesting alternative to avoid hazardous procedures associated to a direct use of gas. The only transition metal  $\eta^2\text{-SiH}_4$  complex  $\text{Mo}(\eta^2\text{-SiH}_4)(\text{CO})(\text{R}_2\text{PC}_2\text{H}_4\text{PR}_2)_2$  was reported in 1995 by Luo, Kubas *et al.* This compound was obtained by direct reaction of  $\text{SiH}_4$  on the molybdenum complex  $\text{Mo}(\text{CO})(\text{R}_2\text{PC}_2\text{H}_4\text{PR}_2)_2$ .<sup>2</sup>  $\text{SiH}_4$  *in situ* generation by catalytic redistribution of  $\text{HSi}(\text{OEt})_3$  by  $\text{Cp}_2\text{TiMe}_2$  was exploited by Harrod *et al.*<sup>3</sup> Such alkoxyhydrosilane redistributions were also catalyzed by zirconium and hafnium complexes as shown by Tilley *et al.*<sup>4</sup>

We have recently discovered that redistribution reaction of dihydrogenosilanes can be performed from the bis(dihydrogen) complex  $\text{RuH}_2(\eta^2\text{-H}_2)_2(\text{PCy}_3)_2$  (**1**). This reaction results in the isolation of the dinuclear complex  $\text{Ru}_2\text{H}_4(\mu\text{-}\eta^2\text{:}\eta^2\text{:}\eta^2\text{-SiH}_4)(\text{PCy}_3)_4$  (**2**) characterized by a novel coordination mode of  $\text{SiH}_4$ .<sup>5</sup> Numerous examples of  $\sigma$ -silane complexes have been reported. They are all characterized by the same bonding picture used to classify the well-known class of  $\sigma$ -dihydrogen complexes.<sup>2b</sup> Coordination of the H-H (or H-Si) bond results

from a subtle balance between the  $\sigma$ -donation from the H-H (or H-Si) bond to an empty  $d_\sigma$  orbital and the back donation from the  $\text{M}(\text{d})$  filled orbital of appropriate symmetry to the H-H (or H-Si)  $\sigma^*$  orbital. We have reported in a preliminary communication the characterization of **2** by multinuclear spectroscopies and an X-ray determination of the analogous complex with triisopropylphosphine in place of  $\text{PCy}_3$ .<sup>5</sup> Theoretical DFT/B3LYP calculations have allowed us to understand the bonding nature between  $\text{SiH}_4$  and the two ruthenium atoms. Coordination is achieved through four  $\sigma\text{-Si-H}$  bonds that differ from the classical Chatt, Dewar and Duncanson model. Each interaction involves  $\sigma$ -donation to a ruthenium and back-bonding from the other ruthenium.

In this paper, we will summarize the key properties of **2** and describe its reactivity toward a few substrates,  $\text{CO}$ ,  $\text{CH}_2\text{Cl}_2$ ,  $\text{tBuNC}$  and  $\text{D}_2$ . We then present a new redistribution reaction leading to the dinuclear complex  $(\text{PCy}_3)_2\text{HRu}(\mu\text{-}\eta^2\text{:}\eta^2\text{-H}_2\text{Si}(\text{OMe})_2)_3\text{RuH}(\text{PCy}_3)$  (**3**). The bonding mode of the bridging alkoxy silanes in **3** is ascertained by NMR and structural characterizations, and more particularly by theoretical calculations.

## Results and discussion

### Synthesis and characterization of $\text{Ru}_2\text{H}_4(\mu\text{-}\eta^2\text{:}\eta^2\text{:}\eta^2\text{-SiH}_4)(\text{PCy}_3)_4$ (**2**)

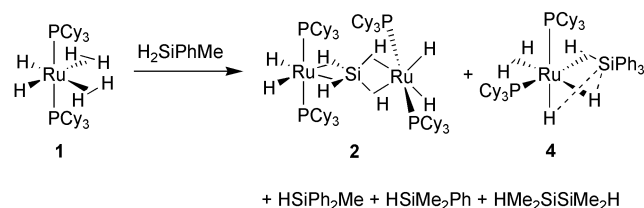
The  $\text{SiH}_4$  dinuclear complex  $(\text{PCy}_3)_2\text{H}_2\text{Ru}(\mu\text{-}\eta^2\text{:}\eta^2\text{:}\eta^2\text{-SiH}_4)\text{-RuH}_2(\text{PCy}_3)_2$  (**2**) is isolated as a white solid in 32% yield by addition at room temperature of 2 equiv. of  $\text{H}_2\text{SiMePh}$  to a suspension of the bis(dihydrogen) complex  $\text{RuH}_2(\eta^2\text{-H}_2)_2(\text{PCy}_3)_2$  (**1**) in pentane. Complex **2** results from the coordination of a  $\text{SiH}_4$  ligand on two dihydridobis(phosphine)ruthenium moieties,  $\text{SiH}_4$  being generated *in situ* by redistribution at silicon. Complex **2** can be obtained from other dihydrogenosilanes such as  $\text{H}_2\text{SiEt}_2$  or  $\text{H}_2\text{SiPh}_2$ , but the more hindered  $\text{H}_2\text{Si}^i\text{Bu}_2$

† Based on the presentation given at Dalton Discussion No. 6, 9–11th September 2003, University of York, UK.

‡ Permanent address: Unité de Recherche de Physico Chimie Moléculaire, Institut Préparatoire des Etudes Scientifiques et Techniques (IPEST), boîte postale 51, 2070 La Marsa, Tunisia.

§ Permanent address: Department of Chemistry, Faculty of Sciences, University Al-Baath, Homs, Syria.

does not react with **1**. The rather low yield (32% for **2**) is explained by the redistribution process depicted in Scheme 1. Several silanes are generated and depending on their reactivity with the ruthenium fragment, the corresponding complexes can be isolated. HSiMePh<sub>2</sub> and HSiMe<sub>2</sub>Ph generated *in situ* remain in solution, whereas HSiPh<sub>3</sub> and SiH<sub>4</sub> are immediately trapped by the ruthenium fragment leading to the formation of RuH<sub>2</sub>(η<sup>2</sup>-H<sub>2</sub>)(η<sup>2</sup>-HSiPh<sub>3</sub>)(PCy<sub>3</sub>)<sub>2</sub> (**4**) and **2**, respectively. The organosilanes were characterized by <sup>1</sup>H NMR and **4** was isolated and separated from **2** by successive crystallization and characterized by NMR.



**Scheme 1** Synthesis of **2** by redistribution reaction.

Complex **4** was previously synthesized by direct reaction of HSiPh<sub>3</sub> to **1** as a result of dihydrogen substitution by the silane.<sup>6</sup> **4** was characterized by X-ray diffraction and DFT/B3LYP calculations. It was the first complex displaying in the coordination sphere of a metal two different σ-bonds (σ-H-H and σ-Si-H) and additional stabilizing secondary interactions between the silicon and the hydrides (SISHA interactions).<sup>7</sup>

As stated in the introduction, characterization of **2** has already appeared in a preliminary form.<sup>5</sup> NMR key features are (i) a nonet at δ 290.2 in the <sup>29</sup>Si INEPT spectrum with *J*(SiH) of 36 Hz in agreement with eight hydrogen atoms, in fast exchange, coupled to the silicon. Such a downfield <sup>29</sup>Si chemical shift could be the signature of a silylene species, as reported in a few complexes,<sup>8,9</sup> but we will see below that it is not the case; (ii) a pseudo-triplet in the <sup>1</sup>H NMR spectrum at δ -7.67 at room temperature (C<sub>7</sub>D<sub>8</sub>). Decoalescence is observed at 203 K leading to two broad signals of equal intensity at δ -6.0 and δ -8.6 at 193 K for the two different types of protons. This facile exchange process is characterized by a Δ*G*<sup>‡</sup> value of 36 kJ mol<sup>-1</sup>.

Single crystals of **2** were obtained and an X-ray determination was undertaken. The data were insufficient to allow the location of the hydrogens around the ruthenium. However, this was possible on crystals of the analogous complex with triisopropylphosphine Ru<sub>2</sub>H<sub>4</sub>(SiH<sub>4</sub>)(P<sup>*i*</sup>Pr<sub>3</sub>)<sub>2</sub> (**2'**) (see Fig. 1 and ref. 5). Complex **2'** was isolated from RuH<sub>2</sub>(H<sub>2</sub>)<sub>2</sub>(P<sup>*i*</sup>Pr<sub>3</sub>)<sub>2</sub> (**1'**) (see Experimental section). Complexes **2** and **2'** display a similar structure with each ruthenium atom in a roughly octahedral geometry. The SiH<sub>4</sub> ligand is trapped between the two RuH<sub>2</sub>(PR<sub>3</sub>)<sub>2</sub> fragments with a linear arrangement of the two

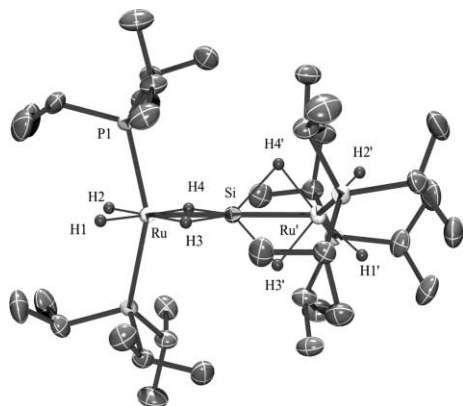


**Fig. 1** X-Ray structure of Ru<sub>2</sub>H<sub>4</sub>(SiH<sub>4</sub>)(P<sup>*i*</sup>Pr<sub>3</sub>)<sub>2</sub> (**2'**). Hydrogen atoms on <sup>*i*</sup>Pr ligands have been omitted for clarity.

**Table 1** Selected DFT/B3LYP optimized geometrical parameters for Ru<sub>2</sub>H<sub>4</sub>(SiH<sub>4</sub>)(PH<sub>3</sub>)<sub>2</sub> (**2''**) and X-ray data for Ru<sub>2</sub>H<sub>4</sub>(SiH<sub>4</sub>)(P<sup>*i*</sup>Pr<sub>3</sub>)<sub>2</sub> (**2'**)<sup>a</sup>

	<b>2''</b>	<b>2'</b>
Ru–H1	1.626	1.49 (2)
Ru–H2	1.626	1.52 (3)
Ru–H3	1.812	1.62 (3)
Ru–H4	1.812	1.62 (3)
Si–H3	1.685	1.69 (3)
Si–H4	1.685	1.73 (3)
Ru–Si	2.229	2.1875 (4)
Ru–P1	2.308	2.3119 (7)
Ru–P2	2.308	2.3129 (7)
P1–Ru–P2	155.4	155.18 (2)
Ru–Si–Ru'	180.0	179.40 (4)
H1–Ru–H2	86.0	86.6 (15)
H3–Ru–H4	95.9	101.4 (14)
H3–Si–H4	105.9	94.2 (14)

<sup>a</sup> See Fig. 1 for labeling of the atoms. Distances are in Å and angles in °.

**Table 2** Natural charges (*q*) and Wiberg bond indices (*W*) for Ru<sub>2</sub>H<sub>4</sub>(SiH<sub>4</sub>)(PH<sub>3</sub>)<sub>4</sub> (**2''**)<sup>a</sup>

	<i>q</i>		<i>W</i>
Ru	-0.88	Ru–Si	0.42
Si	0.95	Ru–H1	0.59
H1	-0.03	Ru–H3	0.21
H3	-0.13	Si–H3	0.58

<sup>a</sup> See Fig. 1 for labeling of the atoms.

ruthenium and silicon atoms. The very short Ru–Si distances of 2.1956(9) Å in **2** and 2.1875(4) Å in **2'** do not correspond to a double Ru=Si bond as it was observed in silylene complexes,<sup>8,9</sup> but are the result of a novel bonding mode.

We have run DFT/B3LYP calculations on the model complex Ru<sub>2</sub>H<sub>4</sub>(SiH<sub>4</sub>)(PH<sub>3</sub>)<sub>2</sub> (**2''**). The optimized structure with *D*<sub>2d</sub> symmetry was found as a minimum on the singlet potential energy surface and confirms the overall structure found by X-ray diffraction for **2** and **2'** (see Table 1). In particular, the Ru–Si distance of 2.229 Å compares well with the X-ray values. The Si–H distances are also in very good agreement (1.685 Å by DFT and 1.71(3) Å av. in **2'**). These DFT Si–H distances represent a lengthening of 13% by comparison to free SiH<sub>4</sub>.

Vibrational spectroscopy can also be a useful tool for the characterization of silane complexes<sup>2b,8</sup> and we have previously shown for the family of the bis(silane) complexes RuH<sub>2</sub>{(η<sup>2</sup>-H-SiR<sub>2</sub>)<sub>2</sub>X}(PR'<sub>3</sub>)<sub>2</sub> that a very good agreement is obtained between experimental and calculated values.<sup>10</sup> σ-Complexes are characterized by a rather strong and broad band in the range 1650–1800 cm<sup>-1</sup>. The IR spectrum of **2** (Nujol mulls) displays a broad band at 1667 cm<sup>-1</sup> and another one at 1911 cm<sup>-1</sup>. These values can be compared to those calculated at the DFT/B3LYP level for **2''**. A b<sub>1</sub> mode for the Ru–H stretching was found at 1996 cm<sup>-1</sup> (intensity: 382 km mol<sup>-1</sup>) and a more intense Ru–H–Si vibration of same symmetry was found at 1605 cm<sup>-1</sup> (intensity: 698 km mol<sup>-1</sup>).

The nature of the ruthenium–silane interaction was studied by a natural bond orbital analysis. We have reported in Table 2 the natural charges *q* and the Wiberg bond indices *W*. The ruthenium carries a negative charge while the silicon is positively charged. The Ru–Si interaction is highly polar with a Wiberg bond index of 0.42. The reduction of the Wiberg index for Ru–H3 (H3 involved in the σ-coordination) by comparison to the value for Ru–H1 (H1 is a classical hydride) indicates a stronger coordination of H3 to Si than to Ru.

Analysis of the molecular orbitals reveals that the bonding interactions between SiH<sub>4</sub> and the two ruthenium fragments occur through the σ-Si–H bonds. In each *xz* and *yz* planes (the *z*

axis is along the two ruthenium and silicon atoms), the two Si–H hybrid orbitals interact with the empty d orbital of one ruthenium center, whereas a back-bonding delocalization occurs from the occupied d orbitals of the other ruthenium center into the  $\sigma^*$  Si–H antibonding orbitals (see Fig. 2). The ruthenium–silane interaction is dominated by the  $\sigma$ -coordination of the ligand to the metal as reflected by the NBO occupancy of each  $\sigma$ -Si–H orbital of 1.71 whereas each  $\sigma^*$  Si–H presents an orbital occupancy of only 0.15. This indicates an overall electron transfer from SiH<sub>4</sub> toward the metallic fragment in agreement with the positive charge of SiH<sub>4</sub> (0.45). A high binding energy of 255 kJ mol<sup>-1</sup> between SiH<sub>4</sub> and the RuH<sub>2</sub>(PH<sub>3</sub>)<sub>2</sub> fragments is calculated.

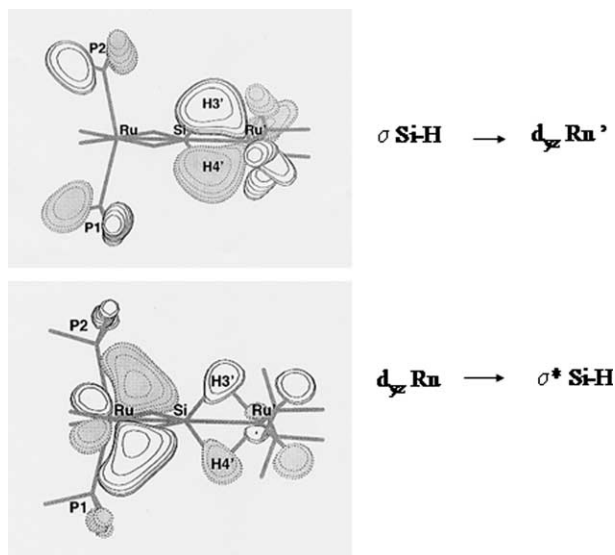
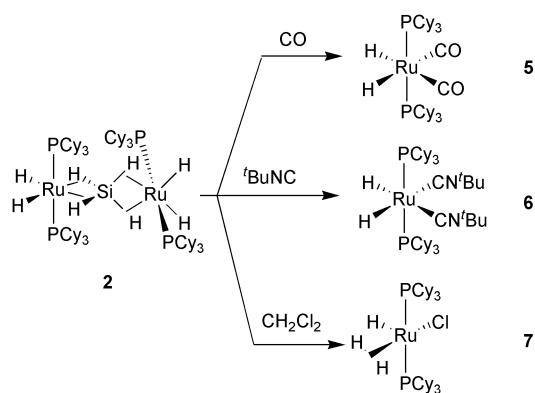


Fig. 2 Isovalue representation of the 4e and 7e valence molecular orbitals of **2**'.

Reactivity studies have now been performed in order to evaluate the chemical reactivity and the stability of the coordinated SiH<sub>4</sub> in complex **2**. The following section describes rather expected reactions whereas in the next one, we report an unprecedented redistribution reaction leading to the isolation of the new complex Ru<sub>2</sub>H<sub>2</sub>( $\mu$ - $\eta^2$ : $\eta^2$ -H<sub>2</sub>Si(OMe)<sub>2</sub>)<sub>3</sub>(PCy<sub>3</sub>)<sub>2</sub> (**3**) with multiple  $\sigma$ -Si–H bonds.

#### Reactivity of **2** with CO, <sup>t</sup>BuNC, CH<sub>2</sub>Cl<sub>2</sub> and D<sub>2</sub>

The reactivity of **2** with CO, <sup>t</sup>BuNC and CH<sub>2</sub>Cl<sub>2</sub> was performed at room temperature in a NMR tube in C<sub>6</sub>D<sub>6</sub> solution, and the fate of the complex was followed by <sup>1</sup>H and <sup>31</sup>P NMR (see Scheme 2). Bubbling CO for 5 min leads to the slow conversion of **2** into the known dicarbonyl complex RuH<sub>2</sub>(CO)<sub>2</sub>(PCy<sub>3</sub>)<sub>2</sub> (**5**).<sup>11</sup> Total conversion into **5** was observed after keeping the tube under CO atmosphere for a day. The reaction between **2**



Scheme 2 Reactivity of **2**.

and <sup>t</sup>BuNC is more complicated and the NMR spectra indicate a mixture of several species. Among them, the formation of RuH<sub>2</sub>(<sup>t</sup>BuNC)<sub>2</sub>(PCy<sub>3</sub>)<sub>2</sub> (**6**) was detected.<sup>10</sup> The spectroscopic data are in agreement with those previously obtained for the direct synthesis of **5** and **6** from **1**.<sup>11,10</sup> Complexes **5** and **6** are in particular characterized by a triplet in <sup>1</sup>H NMR at  $\delta$  -8.07 ( $J(\text{PH}) = 24$  Hz) and  $\delta$  -9.49 ( $J(\text{PH}) = 24$  Hz) and by a singlet in <sup>31</sup>P{<sup>1</sup>H} NMR at  $\delta$  69.0 and  $\delta$  71.3, respectively.

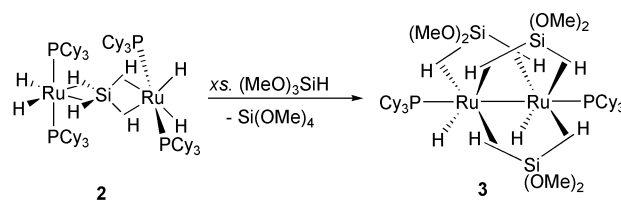
Complex **2** is not stable in the presence of dichloromethane and keeping overnight a CH<sub>2</sub>Cl<sub>2</sub> solution of **2** at room temperature leads to the formation of the chloro complex RuH( $\eta^2$ -H<sub>2</sub>)Cl(PCy<sub>3</sub>)<sub>2</sub> (**7**) identified by a broad signal in <sup>1</sup>H NMR at  $\delta$  -16.45 corresponding to the hydride and the dihydrogen ligand in rapid exchange and by a singlet in the <sup>31</sup>P{<sup>1</sup>H} NMR spectrum at  $\delta$  53.8. As previously published, **7** can also be obtained by direct reaction of dichloromethane with **1**.<sup>11</sup>

Unfortunately in these reactions, the fate of the silane ligand remains unknown. It has not been possible to detect any presence of free SiH<sub>4</sub> (in particular no detection of the characteristic signal at  $\delta$  3.2 in the <sup>1</sup>H NMR spectra) and all our attempts to trap SiH<sub>4</sub> have been unsuccessful. One possible explanation is that the SiH<sub>4</sub> released in the reaction mixture could be adsorbed onto the glassware surface.

We have previously shown that reaction of monosilane or bis(silane) complexes with dihydrogen leads to the elimination of the corresponding silane and formation of the bis(dihydrogen) complex **1**.<sup>6,10</sup> The only exception was with the rigid and very stable disilane RuH<sub>2</sub>[(HSiMe<sub>2</sub>)<sub>2</sub>C<sub>6</sub>H<sub>4</sub>](PCy<sub>3</sub>)<sub>2</sub>. In **2**, strong coordination of the SiH<sub>4</sub> ligand is reflected by its absence of reaction after bubbling H<sub>2</sub> for 10 min or even under 3 bar pressure for 1 h. This observation is also consistent with the calculation of a high binding energy of 255 kJ mol<sup>-1</sup> between SiH<sub>4</sub> and the RuH<sub>2</sub>(PH<sub>3</sub>)<sub>2</sub> fragments. However, after bubbling D<sub>2</sub> for 30 min into a C<sub>6</sub>D<sub>6</sub> solution of **2** a sharp signal appeared at  $\delta$  4.46 indicating the evolution of free H<sub>2</sub> as a result of H/D exchange. When a C<sub>7</sub>D<sub>8</sub> solution of **2** was pressurized to 3 bar of D<sub>2</sub> for 1 h, incorporation of deuterium was observed. Three deuterated isotopomers were characterized by broad signals in the high field region of the <sup>1</sup>H{<sup>31</sup>P} at  $\delta$  -7.63, -7.58 and -7.53. These values correspond to a positive isotopic shift of max 140 ppb, thus shifted at lower field compared to the non-deuterated complex.<sup>12</sup> Low-temperature NMR spectra showed only two broad signals at  $\delta$  -6.3 and  $\delta$  -8.7 of the same intensity indicating that there is no preferred site for deuteration between the two types of hydrogens Ru–H and  $\eta^2$ -H–Si. This H/D exchange is in favour of the involvement of a dihydrogen species in the fast exchange process observed between the eight hydrogens in **2**. This process is characterized by a rather small barrier of 36 kJ mol<sup>-1</sup> at 203 K.

#### Reaction of **2** with HSi(OMe)<sub>3</sub>, Synthesis and characterization of Ru<sub>2</sub>H<sub>2</sub>( $\mu$ - $\eta^2$ : $\eta^2$ -H<sub>2</sub>Si(OMe)<sub>2</sub>)<sub>3</sub>(PCy<sub>3</sub>)<sub>2</sub> (**3**)

No reaction was observed between **2** and alkyl or aryl silanes such as HSiEt<sub>3</sub> or HSiPh<sub>3</sub> but addition of 4 equiv. of HSi(OMe)<sub>3</sub> to a pentane suspension of **2** results in the formation of a ter( $\mu$ - $\eta^2$ : $\eta^2$ -alkoxysilane) complex Ru<sub>2</sub>H<sub>2</sub>( $\mu$ - $\eta^2$ : $\eta^2$ -H<sub>2</sub>Si(OMe)<sub>2</sub>)<sub>3</sub>(PCy<sub>3</sub>)<sub>2</sub> (**3**) isolated as a white solid in 65% yield (see Scheme 3). Silane redistribution occurs slowly at room temperature, the reaction being complete after 3 days.



Scheme 3 Synthesis of **3** by redistribution reaction.

The  $^1\text{H}$  NMR spectrum of **3** in  $\text{C}_6\text{D}_6$  solution at room temperature in the hydride region exhibits a doublet at  $\delta -9.94$  ( $J(\text{PH}) = 11$  Hz) that transforms into a singlet upon phosphorus decoupling with the satellites due to coupling to silicon ( $J(\text{SiH}) = 22$  Hz). The intensity of the silicon satellites suggests the presence of more than one silicon coupled to the hydrides in the molecule. The methyl groups of the methoxy ligands resonate as a singlet at  $\delta 3.90$  integrating for 18H with silicon satellites ( $J(\text{SiH}) = 5$  Hz). Upon coordination, the methyl protons are deshielded (free  $\text{HSi}(\text{OMe})_3$  is observed at  $\delta 3.36$ ). Upon cooling at 213 K in  $\text{C}_7\text{D}_8$  solution, no modification of the hydride signal was observed, and further cooling only led to some broadening. The  $\text{C}_7\text{D}_8$  solution of **3** is stable up to 343 K. The  $^{31}\text{P}\{^1\text{H}\}$  NMR spectrum exhibits one resonance at  $\delta 79.30$  with satellites due to the silicon coupling ( $J(\text{SiP}) = 15$  Hz). The selective decoupling of the  $\text{PCy}_3$  protons allows the quantification of the hydrides coupled to phosphorus. The  $^{31}\text{P}\{^1\text{H}_{\text{PCy}_3}\}\{^{29}\text{Si}\}$  NMR spectrum shows a quintet with a coupling constant of 11 Hz, which is in agreement with four hydrogen atoms coupled to a phosphorus. The  $^{29}\text{Si}\{^1\text{H}\}\{^{31}\text{P}\}$  spectrum exhibits a singlet at  $\delta 85.74$ . This resonance is shifted to high field compared to complex **2** and is now in a normal range of values found for  $\sigma\text{-Si-H}$  complexes.<sup>8</sup>

The  $^{29}\text{Si}\{^1\text{H}\{^1\text{H}_{\text{OMe}}\}\{^{31}\text{P}\}$  INEPT NMR spectrum shows a nonet ( $J(\text{SiH}) = 22$  Hz) in agreement with eight hydrogen atoms in fast exchange coupled to the silicons (see Fig. 3).

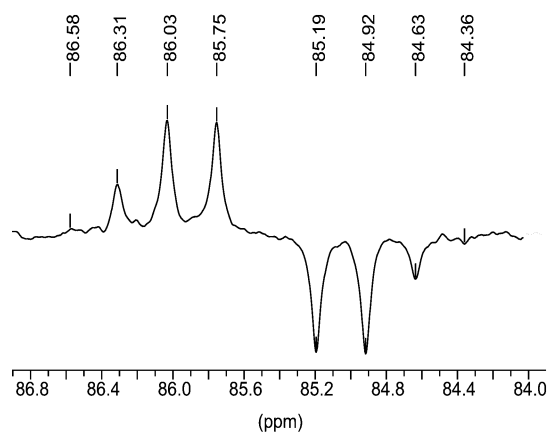


Fig. 3  $^{29}\text{Si}\{^1\text{H}\{^1\text{H}_{\text{OMe}}\}\{^{31}\text{P}\}$  INEPT NMR spectrum of **3**.

We were able to obtain crystals suitable for an X-ray determination. However, as a result of the quality of the crystal, the data do not allow a complete analysis. The molecular structure is shown in Fig. 4. The key features are the nearly colinear arrangement of the two Ru and the two P atoms with  $\text{P}(1)\text{-Ru}(1)\text{-Ru}(2)$  and  $\text{Ru}(1)\text{-Ru}(2)\text{-P}(2)$  angles of  $174.16$  (7) and  $179.55$  (7) $^\circ$ , respectively. The  $\text{Ru}(1)\text{-Ru}(2)$  bond distance of  $2.8529$  (10)  $\text{\AA}$  is compatible with a metal-metal bond.<sup>13</sup> In

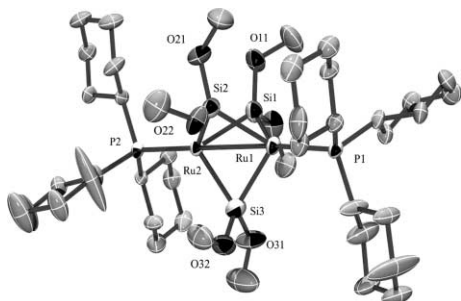


Fig. 4 X-Ray structure of  $\text{Ru}_2\text{H}_2(\text{H}_2\text{Si}(\text{OMe})_2)_3(\text{PCy}_3)_2$  (**3**). Selected bond lengths ( $\text{\AA}$ ) and angles ( $^\circ$ ):  $\text{Ru}1\text{-P}1$  2.331(2),  $\text{Ru}2\text{-P}2$  2.329(2),  $\text{Ru}1\text{-Ru}2$  2.8529(10),  $\text{Ru}1\text{-Si}1$  2.456(3),  $\text{Ru}1\text{-Si}2$  2.408(3),  $\text{Ru}1\text{-Si}3$  2.355(3),  $\text{Ru}2\text{-Si}1$  2.364(3),  $\text{Ru}2\text{-Si}2$  2.419(3),  $\text{Ru}2\text{-Si}3$  2.408(3);  $\text{P}1\text{-Ru}1\text{-Ru}2$   $174.16$ (7),  $\text{P}2\text{-Ru}2\text{-Ru}1$   $179.55$ (7),  $\text{Ru}1\text{-Si}1\text{-Ru}2$   $72.55$ (8),  $\text{Ru}1\text{-Si}2\text{-Ru}2$   $72.45$ (9),  $\text{Ru}1\text{-Si}3\text{-Ru}2$   $73.57$ (8).

Table 3 Selected optimized geometrical parameters for  $\text{RuH}_2(\mu\text{-H}_2\text{-Si}(\text{OR}')_2)_3(\text{PR}_3)_2$ <sup>a</sup>

	A	A'	B	C	C'
Ru1–Ru2	2.878	2.862	2.899	2.887	2.881
Ru1–Si1	2.483	2.455	2.470	2.486	2.483
Ru2–Si1	2.365	2.352	2.359	2.398	2.399
Ru1–Si2	2.574	2.524	2.555	2.551	2.540
Ru2–Si2	2.574	2.524	2.555	2.551	2.540
Ru1–Si3	2.365	2.352	2.359	2.400	2.400
Ru2–Si3	2.483	2.456	2.470	2.487	2.485
Ru1–H1a	1.693	1.682	1.692	1.690	1.687
Si1–H1a	1.702	1.722	1.714	1.735	1.733
Ru2–H1b	1.661	1.654	1.660	1.669	1.688
Si1–H1b	1.787	1.806	1.806	1.760	1.751
Ru1–H2a	1.732	1.711	1.726	1.751	1.748
Si2–H2a	1.680	1.723	1.694	1.653	1.653
Ru2–H2b	1.732	1.711	1.726	1.751	1.747
Si2–H2b	1.680	1.723	1.694	1.654	1.654
Ru1–H3a	1.661	1.654	1.660	1.669	1.669
Si3–H3a	1.787	1.806	1.806	1.759	1.750
Ru2–H3b	1.693	1.682	1.692	1.689	1.688
Si3–H3b	1.702	1.722	1.714	1.734	1.735
Ru1–H4a	1.640	1.639	1.644	1.638	1.627
Ru2–H4b	1.640	1.639	1.644	1.638	1.627
P1–Ru1–Ru2	175.22	174.29	176.36	174.53	174.45
P2–Ru2–Ru1	175.21	174.24	176.36	174.60	174.50
Ru1–Si1–Ru2	72.79	73.04	73.73	72.44	72.33
Ru1–Si2–Ru2	67.97	69.08	69.13	68.92	69.11
Ru1–Si3–Ru2	72.78	73.04	73.72	72.39	72.26
P1–Ru1–H4a	82.31	81.95	82.82	81.03	81.08
P2–Ru2–H4b	82.31	81.92	82.81	81.00	81.03

<sup>a</sup> See Fig. 5 for labeling of the atoms. Distances are in  $\text{\AA}$  and angles in  $^\circ$ . A:  $\text{R} = \text{R}' = \text{H}$ ; DFT/B3LYP. A':  $\text{R} = \text{R}' = \text{H}$ ; DFT/B3PW91. B  $\text{R} = \text{Me}$ ,  $\text{R}' = \text{H}$ ; DFT/B3LYP. C:  $\text{R} = \text{H}$ ,  $\text{R}' = \text{Me}$ ; DFT/B3LYP. C':  $\text{R} = \text{H}$ ,  $\text{R}' = \text{Me}$ ; DFT/B3LYP with f orbital contributions.

agreement with NMR data, only two methoxy groups remain coordinated on a silicon and three  $\text{Si}(\text{OMe})_2$  groups are bridging the two ruthenium atoms. The  $\text{Ru}\text{-Si}$  distances are in the range  $2.35\text{--}2.46$   $\text{\AA}$ , thus typically the range found for silyl or  $\sigma\text{-Si-H}$  complexes.<sup>8</sup> The  $\text{Ru}\text{-Si}\text{-Ru}$  angles are close to  $73^\circ$ .

If there is no doubt for a formulation of a dinuclear complex with only one phosphine coordinated to each ruthenium and three bridging  $\text{Si}(\text{OMe})_2$  groups, the main question concerns the mode of coordination of the bridging silanes and of the eight hydrogens (as detected by NMR) around the coordination sphere of the metals. In the absence of better X-ray data, the use of theoretical calculations is particularly informative.<sup>14,15</sup> We have thus performed DFT calculations on the model complex  $\text{Ru}_2\text{H}_2(\mu\text{-H}_2\text{Si}(\text{OR}')_2)_3(\text{PR}_3)_2$ . Complexes **A**, **B** and **C** corresponding to the three cases  $\text{R}' = \text{R} = \text{H}$  for (**A**),  $\text{R}' = \text{H}$ ,  $\text{R} = \text{Me}$  for (**B**) and  $\text{R}' = \text{Me}$ ,  $\text{R} = \text{H}$  for (**C**) have been optimized using the B3LYP hybrid functional. Values of selected geometrical parameters are listed in Table 3.

The overall B3LYP-optimized geometry does not change significantly when using  $\text{PMe}_3$  instead of  $\text{PH}_3$  (**B** to **A**) or  $\text{H}_2\text{Si}(\text{OMe})_2$  instead of  $\text{H}_2\text{Si}(\text{OH})_2$  (**C** to **A**). In the three cases, one silicon ( $\text{Si}2$ ) is located at an equal distance from  $\text{Ru}1$  and  $\text{Ru}2$  whereas the other silicons are bridging unsymmetrically the metals in a reciprocal manner. To simplify the discussion, we will only comment the values obtained for the model complex **A**. The  $\text{Ru}\text{-Si}$  distances are in the range  $2.35\text{--}2.57$   $\text{\AA}$ . They can be classified as  $d(\text{Ru}1\text{-Si}3) = d(\text{Ru}2\text{-Si}1) < d(\text{Ru}1\text{-Si}1) = d(\text{Ru}2\text{-Si}3) < d(\text{Ru}1\text{-Si}2) = d(\text{Ru}2\text{-Si}2)$ . It should be noted that the highest values of  $2.57$   $\text{\AA}$  involving the  $\text{Si}2$  atom lie among the highest X-ray values reported for  $\sigma\text{-Si-H}$  ruthenium complexes ( $2.30\text{--}2.68$   $\text{\AA}$ ).<sup>8,13</sup> Each silane is coordinated to the two ruthenium *via* two  $\text{Si-H}$  bonds presenting different activation modes. The bonds involving  $\text{Si}1$  namely  $\text{Si}1\text{-H}1\text{a}$  and  $\text{Si}1\text{-H}1\text{b}$ , are lengthened by 14 and 20%, respectively, by comparison to the optimized  $\text{Si-H}$  bond length in free  $\text{SiH}_2(\text{OH})_2$  ( $1.49$   $\text{\AA}$ ).

**Table 4** Natural charges ( $q$ ) and Wiberg bond indices ( $W$ ) for  $\text{Ru}_2\text{H}_2(\mu\text{-H}_2\text{Si}(\text{OMe})_2)_3(\text{PH}_3)_2$  (**C**)<sup>a</sup>

$q$		$W$	
Ru1	-0.98	Ru1-Si1	0.26
Ru2	-0.98	Ru1-Si2	0.21
Si1	1.89	Ru1-Si3	0.32
Si2	1.87	Ru1-H1a	0.35
Si3	1.89	Ru1-H2a	0.23
H1a	-0.11	Ru1-H3a	0.38
H1b	-0.06	Si1-H1a	0.37
H2a	-0.16	Si1-H1b	0.35
H2b	-0.16	Si2-H2a	0.49
H3a	-0.06	Si2-H2b	0.49
H3b	-0.11	Si3-H3a	0.35
H4a	-0.04	Si3-H3b	0.37
H4b	-0.04	Ru1-H4a	0.54
		Ru1-Ru2	0.13

<sup>a</sup> See Fig. 5 for labeling of the atoms.

Symmetrical values have been obtained for the lengthening of the Si3-H bonds (20% for Si3-H3a and 14% for Si3-H3b). As expected from the Ru-Si2 distances, the lengthening of the Si2-H bonds is smaller than 13%. This can be attributed to the *trans* position with the hydrides H4a and H4b. The same situation is observed in complex **2'** (see above): a lengthening of 13% for the  $\sigma$ -Si-H bonds was calculated by comparison to the DFT values for free  $\text{SiH}_4$ .

Similar results have been obtained for the optimization of  $\text{Ru}_2\text{H}_2(\mu\text{-H}_2\text{Si}(\text{OH})_2)_3(\text{PH}_3)_2$  but using the B3PW91 functional (see column A' in Table 3). Moreover, we have tested the effect of f orbital contributions on isomer C. The results are reported in column C' and show no noticeable difference.

The nature of the ruthenium-silane interactions was also studied by a natural bond orbital analysis. We have reported in Table 4 the natural charges ( $q$ ) and the Wiberg bond indices ( $W$ ) for C. As for complex **2'**, the ruthenium carries a negative charge while the silicon is positive. However, the charges on the silicon atoms in C are much more important than in **2'** due to the presence of OMe substituents. Indeed, the oxygen atoms are negatively charged with  $q = -0.98$ . The hydrogen atoms around the metal are negatively charged with the two classical hydrides having the smallest value (-0.04). The highest values are obtained for the hydrogens bound to Si2. We have only reported in Table 4 the Wiberg bond indices involving Ru1. Those concerning Ru2 can be easily deduced as a result of symmetrical considerations (see discussion above for the Ru-Si distances).

The six Ru-Si interactions are characterized by bond index values (0.21 to 0.32) slightly smaller or similar than that calculated for other  $\sigma$ -silane complexes. For example, we have found for  $\text{RuH}_2(\text{H}_2)(\text{HSiH}_3)(\text{PH}_3)_2$  the model complex of  $\text{RuH}_2(\text{H}_2)(\text{HSiPh}_3)(\text{PCy}_3)_2$  (**4**) a value of 0.31 and in the case of the bis(silane) complex  $\text{RuH}_2[(\text{HSiH}_2)_2(\text{C}_6\text{H}_4)](\text{PH}_3)_2$  a similar value was also obtained (0.29).<sup>16</sup> However, a higher value (0.42) was calculated for **2'**. The Si-H Wiberg indices are of course reduced (0.35 to 0.49) compared to the value calculated for free  $\text{H}_2\text{Si}(\text{OMe})_2$  (0.89). The Wiberg indices of Ru1 with the three hydrogens H1a, H2a and H3a involved in the  $\sigma$ -Si-H coordination are reduced (0.23 to 0.38) by comparison to the value for Ru1-H4a (0.54) involving the classical hydride. H1a appears to be equally bonded to Ru1 and Si1 with two similar Wiberg indices of 0.35 and 0.37 for Ru1-H1a and Si1-H1a, respectively. The same situation can be observed for H3a bridging Ru1 and Si3. In the contrary, the Wiberg indices involving H2a (0.23 for Ru1-H2a and 0.49 for Si2-H2a) indicate a stronger coordination of H2a to the silicon. A similar result is found for **2'** (0.21 for Ru-H3 and 0.58 for Si-H3). Finally, the Ru1-Ru2 Wiberg index is small (0.13). We have postulated for **3** the existence of a metal-metal bond in agreement with the X-ray Ru-Ru distance of 2.8529(10) Å and with the diamagnet-

ism of the compound. It is worth noting that a similar distance is calculated by DFT (2.86 to 2.90 Å for A to C'). We will examine in a future study the validity of NBO analysis for the evaluation of a metal-metal interaction before any conclusion on this specific case.

The geometry described in Scheme 3 and Fig. 5 is in agreement with all our data. Each bridging  $\text{H}_2\text{Si}(\text{OMe})_2$  silane is coordinated to the two ruthenium *via* a  $\sigma$ -Si-H bond. The coordination sphere of each ruthenium can be viewed as an octahedron with the apical positions occupied by a phosphine and the other ruthenium. Three  $\sigma$ -Si-H bonds and a hydride occupy the equatorial sites. The presence of a single Ru-Ru bond would be in agreement with a diamagnetic compound. However, such a picture bonding should be only considered as an *arrested stage of a more delocalized system involving all the Ru, Si and H atoms*.

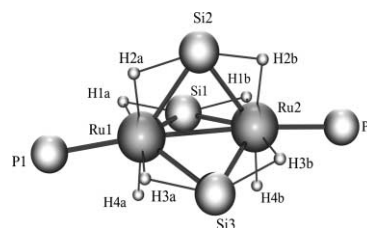


**Fig. 5** DFT/B3LYP optimized structure of  $\text{Ru}_2\text{H}_2(\mu\text{-H}_2\text{Si}(\text{OMe})_2)_3(\text{PH}_3)_2$  (**C**); OMe groups and hydrogens on phosphorus have been omitted for clarity.

It is remarkable that the complex published in 1969 by Graham *et al.*, that can be considered as the first complex presenting strong evidence for a  $\sigma$ -Si-H coordination, is a dinuclear complex with a bridging  $\eta^2\text{-}\eta^2\text{-H}_2\text{SiPh}_2$  ligand.<sup>17</sup> More than 35 years later, the first X-ray structure on an analogous dinuclear ruthenium species with location of the hydrogens atoms and detailed multinuclear NMR analysis were reported by Suzuki *et al.*<sup>13</sup> This compound  $[\text{Cp}^*\text{Ru}(\text{CO})]_2(\mu\text{-}\eta^2\text{-}\eta^2\text{-H}_2\text{Si}^t\text{Bu}_2)$  displays a Ru-Ru bond distance of 2.9638(8) Å. The two  $3c\text{-}2e^-$  Si-H bonds are supported both by X-ray and NMR data with in particular Si-H distances of 1.76 Å (av.) and  $J(\text{SiH})$  of 22.4 Hz. This  $J$  value is in the lower limit of what is normally found for  $\sigma$ -Si-H bonds<sup>8,26,10</sup> but is explained by the presence of the carbonyl ligand. In the related complex  $[\text{Cp}^*\text{Ru}(\mu\text{-H})]_2(\mu\text{-}\eta^2\text{-}\eta^2\text{-H}_2\text{Si}^t\text{Bu}_2)$  an apparent  $J(\text{SiH})$  value of 34.2 Hz was measured. In this later case the apparent constant is an average value as the two hydrides and the hydrogens of the bridging ligand are in rapid exchange.<sup>13</sup> In our system, the apparent value of 22 Hz obtained for **3** represents an average between the  $^2J(\text{SiH})$  involving the terminal hydrides and the  $^1J(\text{SiH})$  for  $\sigma$ -Si-H.

In order to get more information on the mechanism of the redistribution process leading to the obtention of **3** from  $\text{HSi}(\text{OMe})_3$  and **2** which contains a  $\text{SiH}_4$  ligand, we have monitored by NMR the addition of 4 equiv. of  $\text{HSi}(\text{OMe})_3$  to **2**. The only organometallic complexes present in the reaction mixture all along the course of the reaction are **2** and **3**. Elimination of  $\text{PCy}_3$  from **2** was confirmed by the observation of an increasing signal at  $\delta$  10 characteristic of free phosphine in the  $^{31}\text{P}$  NMR spectrum. Moreover, the missing methoxy group in the bridging ligand **3** is recovered as  $\text{Si}(\text{OMe})_4$  that we were able to detect in the reaction mixture.  $\text{Si}(\text{OMe})_4$  is characterized by a singlet at  $\delta$  3.47 in the  $^1\text{H}$  NMR spectrum.

## Conclusion

Reactions of silanes with the bis(dihydrogen) complex  $\text{RuH}_2(\eta^2\text{-H}_2)(\text{PCy}_3)_2$  (**1**) lead to a versatile chemistry with a wide variety of silane bonding modes and multiple redistribution processes. We have reported the result of two successive silane redistributions. The first reaction leads in the case of  $\text{H}_2\text{SiMePh}$

to an extensive redistribution process of all the silane substituents. We were able to isolate two organometallic species **2** and **4**.  $\text{RuH}_2(\eta^2\text{-H}_2)(\eta^2\text{-HSiPh}_3)(\text{PCy}_3)_2$  (**4**) was previously characterized as the first complex displaying in the coordination sphere of a metal two different  $\sigma$ -bonds ( $\sigma\text{-H-H}$  and  $\sigma\text{-Si-H}$ ) and additional stabilizing secondary interactions between the silicon and the hydrides (SISHA interactions).<sup>6,7</sup> The remarkable  $\text{SiH}_4$  complex  $(\text{PCy}_3)_2\text{Ru}(\mu\text{-}\eta^2\text{:}\eta^2\text{:}\eta^2\text{-SiH}_4)\text{RuH}_2(\text{PCy}_3)_2$  (**2**) presents a new silane coordination mode achieved through four  $\sigma\text{-Si-H}$  bonds. This mode differs from the classical Chatt, Dewar and Duncanson model. Each interaction involves  $\sigma$ -donation to a ruthenium and back-bonding from the other ruthenium. This  $\text{SiH}_4$  ligand is strongly bonded to the metals but can be evolved under CO atmosphere or in chlorinated solvent for example. Interestingly, **2** is stable under dihydrogen atmosphere but H/D exchange can be observed. We have no key information on the mechanism leading to Si-C bond cleavages, but it seems that migration of the silicon-attached groups occurs by direct transfer of a substituent to another silicon. This transfer is assisted by the metal, allowing the generation of an electrophilic silicon center. Formation of the volatile  $\text{SiH}_4$  is the driving force of the reaction.

The second redistribution reaction is obtained by adding  $\text{HSi}(\text{OMe})_3$  to the  $\text{SiH}_4$  complex **2**. The new dinuclear complex  $\text{Ru}_2\text{H}_2(\mu\text{-}\eta^2\text{:}\eta^2\text{-H}_2\text{Si}(\text{OMe})_2)_3(\text{PCy}_3)_2$  (**3**) is isolated in good yield and characterized by multinuclear NMR and X-ray diffraction. Here again, theoretical studies were decisive to locate the hydrogen atoms around the coordination sphere of the metals and to propose a bonding picture of the molecule taking into account all the data. The coordination sphere of each ruthenium is occupied by three  $\sigma\text{-Si-H}$  bonds from the bridging  $\text{H}_2\text{Si}(\text{OMe})_2$  silanes, a hydride, a phosphine and the other ruthenium. However, such a picture bonding should be only considered as an arrested stage of a more delocalized system involving all the Ru, Si and H atoms. Indeed, the structural parameters (Ru-Si, Si-H bond distances) and the NBO data (Wiberg bond indices) serve as good indicators of the strength of the metal-silane interaction. However, the frontiers between true  $\sigma\text{-M-H-Si}$  interactions and more delocalized systems with strong to weak interactions between the three atoms are not clear-cut, specially in the presence of multiple interactions.

## Experimental

### General procedures

All reactions and workup procedures were performed under an argon atmosphere using conventional vacuum line and Schlenk tube techniques. Solvents were dried and freshly distilled according to standard procedures and degassed prior to use.  $\text{Ru}(\text{COD})(\text{COT})$  and  $\text{RuH}_2(\text{H}_2)_2(\text{PCy}_3)_2$  (**1**) were prepared according to published procedures.<sup>18</sup> All NMR solvents were dried and degassed using appropriated methods. NMR spectra were acquired on Bruker AC 200 and AMX 400 spectrometers. Microanalysis were performed by the Laboratoire de Chimie de Coordination Microanalytical Service. Infrared spectra were obtained as Nujol mulls on a Perkin-Elmer 1725 FT-IR spectrometer.

### Synthesis and characterization of $\text{Ru}_2\text{H}_4(\mu\text{-}\eta^2\text{:}\eta^2\text{:}\eta^2\text{-SiH}_4)(\text{PCy}_3)_4$ (**2**)

Addition at room temperature of  $\text{H}_2\text{SiMePh}$  (124  $\mu\text{L}$ ; 0.90 mmol) to a suspension of  $\text{RuH}_2(\text{H}_2)_2(\text{PCy}_3)_2$  (**1**) (300 mg; 0.45 mmol) in pentane, resulted in immediate gas evolution. The mixture turned orange and was stirred for 3 h at room temperature leading to the formation of a white solid. This was collected by filtration and was washed twice with pentane and dried under argon and finally under vacuum. Complex **2** was obtained in 32% yield. Anal. Calc. for  $\text{Ru}_2\text{C}_{72}\text{H}_{140}\text{P}_4\text{Si}$ : C, 63.59; H, 10.38. Found: C, 63.03; H, 10.45%.  $^1\text{H}$  NMR (400 MHz,

$\text{C}_6\text{D}_6$ , 293 K):  $\delta$  -7.67 (pt, 8H), 1.2–2.4 (m, 132 H,  $\text{PCy}_3$ ). 193 K:  $\delta$  -6.0 (br, 4H), -8.6 (br, 4H).  $^{29}\text{Si}$  INEPT  $^1\text{H}$  coupled (79.5 MHz,  $\text{C}_6\text{D}_6$ , 288 K):  $\delta$  290.2 (nonet,  $J_{\text{Si-H}} = 36$  Hz);  $^{29}\text{Si}\{^1\text{H}\}$   $\delta$  290.2 (s);  $^{31}\text{P}\{^1\text{H}\}$  NMR (81 MHz,  $\text{C}_6\text{D}_6$ ):  $\delta$  72.27 (s). IR (Nujol) 1667  $\text{cm}^{-1}$  (br,  $\nu\text{Ru-H-Si}$ ) 1911  $\text{cm}^{-1}$  (br,  $\nu\text{Ru-H}$ ).

The remaining filtrate was kept at room temperature. A beige solid was then obtained in 40% yield and characterized by NMR as  $\text{RuH}_2(\eta^2\text{-H}_2)(\eta^2\text{-HSiPh}_3)(\text{PCy}_3)_2$  (**4**):  $^1\text{H}$  NMR (200 MHz,  $\text{C}_6\text{D}_6$ , 298 K):  $\delta$  8–7 (m, Ph), 1.1–2.4 (m,  $\text{PCy}_3$ ), -8.45 (s, br, RuH).  $^{31}\text{P}\{^1\text{H}\}$  NMR (81 MHz,  $\text{C}_6\text{D}_6$ ):  $\delta$  59.8 (s).

### NMR characterization of the redistribution products

Two equiv. of  $\text{H}_2\text{SiMePh}$  were added to a  $\text{C}_6\text{D}_6$  suspension of **1** in a NMR tube. Immediate gas evolution and dissolution of the mixture were observed. The resulting solution was analyzed by  $^1\text{H}$  and  $^{31}\text{P}$  NMR. The spectra showed the total conversion of **1** and  $\text{H}_2\text{SiMePh}$ , and formation of **3** and **4** in a ratio 1 : 1.3 and of  $\text{HSiMePh}_2$  :  $\text{HSiMe}_2\text{Ph}$  in a ratio 2.2 : 3.4 whereas only traces of  $\text{HMe}_2\text{SiSiMe}_2\text{H}$  were detected.

$\text{H}_2\text{SiMePh}$ :  $^1\text{H}$  NMR (200 MHz,  $\text{C}_6\text{D}_6$ , 298 K):  $\delta$  8–7 (m, 5H, Ph), 4.49 (q, 2H, SiH,  $J_{\text{H-H}} = 4.3$  Hz), 0.18 (t, 3 H, Me,  $J_{\text{H-H}} = 4.3$  Hz).

$\text{HSiMePh}_2$ :  $^1\text{H}$  NMR (200 MHz,  $\text{C}_6\text{D}_6$ , 298 K):  $\delta$  8–7 (m, 10H, Ph), 5.14 (q, 1H, SiH,  $J_{\text{H-H}} = 3.9$  Hz), 0.46 (d, 3 H, Me,  $J_{\text{H-H}} = 3.9$  Hz).

$\text{HSiMe}_2\text{Ph}$ :  $^1\text{H}$  NMR (200 MHz,  $\text{C}_6\text{D}_6$ , 298 K):  $\delta$  8–7 (m, 5H, Ph), 4.63 (s, 1H, SiH,  $J_{\text{H-H}} = 3.8$  Hz), 0.21 (d, 6 H, Me,  $J_{\text{H-H}} = 3.8$  Hz).

$\text{HMe}_2\text{SiSiMe}_2\text{H}$ :  $^1\text{H}$  NMR (200 MHz,  $\text{C}_6\text{D}_6$ , 298 K):  $\delta$  4.17 (sept, 2H, SiH,  $J_{\text{H-H}} = 3.9$  Hz), 0.01 (d, 12 H, Me,  $J_{\text{H-H}} = 3.9$  Hz).

### Synthesis and characterization of $\text{Ru}_2\text{H}_4(\mu\text{-}\eta^2\text{:}\eta^2\text{:}\eta^2\text{-SiH}_4)(\text{P}^i\text{Pr}_3)_4$ (**2'**)

The bis(dihydrogen) precursor  $\text{RuH}_2(\text{H}_2)_2(\text{P}^i\text{Pr}_3)_2$  was generated *in situ* by adding two equiv. of  $\text{P}^i\text{Pr}_3$  (303  $\mu\text{L}$ ; 1.59 mmol) to a solution of  $\text{Ru}(\text{COD})(\text{COT})$  (250 mg; 0.79 mmol) in pentane under 3 bar of dihydrogen. After 3 h of stirring and depressurization under argon, 2 equiv. of  $\text{H}_2\text{SiPhMe}$  (218.5  $\mu\text{L}$ ; 1.59 mmol) were added. After stirring overnight, the solution was placed at -30 °C and the resulting pale yellow crystals were collected by filtration (yield *ca.* 10%).  $^1\text{H}$  NMR (200 MHz,  $\text{C}_6\text{D}_6$ , 296 K):  $\delta$  -7.75 (pt, 8H), 1.3 (m, 72H,  $\text{P}^i\text{Pr}_3$ ), 2.0 (m, 12H,  $\text{P}^i\text{Pr}_3$ );  $^{31}\text{P}\{^1\text{H}\}$  NMR (81 MHz,  $\text{C}_6\text{D}_6$ ):  $\delta$  88.68 (s).

The crystal data for **2'** were reported in the preliminary communication.<sup>5</sup>

### Synthesis and characterization of $\text{Ru}_2\text{H}_2(\mu\text{-}\eta^2\text{:}\eta^2\text{-H}_2\text{Si}(\text{OMe})_2)_3(\text{PCy}_3)_2$ (**3**)

$\text{HSi}(\text{OMe})_3$  (78  $\mu\text{L}$ ; 0.580 mmol) was added at room temperature to a suspension of  $\text{Ru}_2\text{H}_4(\mu\text{-}\eta^2\text{:}\eta^2\text{:}\eta^2\text{-SiH}_4)(\text{PCy}_3)_4$  (**2**) (200 mg; 0.145 mmol) in pentane (25 mL). The reaction mixture was stirred for 3 days at room temperature. The resulting white solid was collected by filtration, washed with pentane, and dried under vacuum (yield 65%). Anal. Calc. for  $\text{Ru}_2\text{H}_2(\text{H}_2\text{Si}(\text{OMe})_2)_3(\text{PCy}_3)_2\text{Si}(\text{OMe})_4$ :  $\text{Ru}_2\text{C}_{46}\text{H}_{104}\text{O}_{10}\text{P}_2\text{Si}_4$ : C, 46.27; H, 8.72. Found C, 46.67; H, 8.63%. Integration of the  $^1\text{H}$  NMR spectrum of a  $\text{C}_6\text{D}_6$  solution of **3** confirms the presence of 1 equiv. of  $\text{Si}(\text{OMe})_4$  (singlet at 3.47 ppm) for 1 equiv. of **3**.

$^1\text{H}$  NMR (400 MHz,  $\text{C}_6\text{D}_6$ , 293 K):  $\delta$  3.90 (18H, s, OMe), 2.3–1.3 (66H, m,  $\text{PCy}_3$ ) and -9.94 (8H, d,  $J_{\text{P-H}} = 11$  Hz, Ru-H).  $^{31}\text{P}$  NMR (162 MHz,  $\text{C}_6\text{D}_6$ , 293 K):  $\delta$  78.3 (s).  $^{31}\text{P}\{^1\text{H}_{\text{PCy}_3}\}\{^{29}\text{Si}\}$  NMR (162 MHz,  $\text{C}_6\text{D}_6$ , 293 K):  $\delta$  78.3 (quintet,  $J_{\text{P-H}} = 11$  Hz).  $^{29}\text{Si}$  NMR (inept  $^{29}\text{Si-H}\{^1\text{H}_{\text{OMe}}\}\{^{31}\text{P}\}$  non-refocused; 79.5 MHz;  $\text{C}_6\text{D}_6$ ) 85.5 (nonet,  $J_{\text{Si-H}} = 22$  Hz). IR (Nujol) 1703  $\text{cm}^{-1}$  (br,  $\nu\text{Ru-H-Si}$ ) 1899  $\text{cm}^{-1}$  (br,  $\nu\text{Ru-H}$ ) 2022  $\text{cm}^{-1}$  (br,  $\nu\text{Ru-H}$ ).

## Crystallography

Data for **3** were collected at low temperature ( $T = 180$  K) on a Stoe Imaging Plate Diffraction System (IPDS) equipped with an Oxford Cryosystems cryostream cooler device and using graphite-monochromated Mo- $K\alpha$  radiation ( $\lambda = 0.71073$  Å). The final unit cell parameters were obtained by least-squares refinement of a set of 8000 well measured reflections, and crystal decay was monitored by measuring 200 reflections by image. No significant fluctuation of the intensities was observed. The structure was solved by direct methods using the program SIR92,<sup>19</sup> and refined by least-squares procedures on  $F^2$  by using SHELXL-97<sup>20</sup> integrated in the package WINGX version 1.64.<sup>21</sup> Hydrogen atoms were located on a difference Fourier map but introduced in idealized positions, their positional parameters were calculated with C–H distances fixed (0.93 Å) for  $sp^2$  C and (0.96 Å) for  $sp^3$  and with  $U_{iso}$  fixed of 1.2 times the  $U_{eq}$  value of the attached  $sp^2$  C and 1.5 times the  $U_{eq}$  values of the attached  $sp^3$  C atom. The last difference Fourier syntheses indicated some residual peaks of electronic densities which appeared to be spread and diffuse. They were located close to the  $-\text{Si}(\text{OCH}_3)_2$  ligands. It was impossible to relate these peaks with any convenient model or disorder and all attempts to model these densities have failed. All non-hydrogen atoms were anisotropically refined and in the last cycles of refinement a weighting scheme was used. Weights are calculated from the following formula:  $w = 1/[\sigma^2(F_o^2) + (aP)^2 + bP]$  where  $P = (F_o^2 + 2F_c^2)/3$ . Drawing of the molecule was performed using the program ORTEP3 with 40% probability displacement ellipsoids for non-hydrogen atoms and printed by using the Pov-ray software.<sup>22</sup>

Crystal data for **2**:  $\text{C}_{72}\text{H}_{132}\text{P}_4\text{SiRu}_2$ ,  $M = 1351.89$ , orthorhombic, space group  $Pbcn$ ,  $T = 160(2)$  K,  $a = 15.831(2)$ ,  $b = 19.063(2)$ ,  $c = 24.035(3)$  Å,  $V = 7253.3(17)$  Å<sup>3</sup>,  $Z = 4$ ,  $\mu = 0.559$  mm<sup>-1</sup>, reflections collected/unique = 29110/3755,  $R1 = 0.0970$ ,  $wR2 = 0.1599$ , GOF = 0.860.

Crystal data for **3**:  $\text{C}_{42}\text{H}_{84}\text{O}_6\text{P}_2\text{Si}_3\text{Ru}_2$ ,  $M = 1033.44$ , triclinic, space group  $P\bar{1}$ ,  $T = 180(2)$  K,  $a = 9.8062(12)$ ,  $b = 14.959(2)$ ,  $c = 18.710(3)$  Å,  $\alpha = 93.103(17)$ ,  $\beta = 99.303(16)$ ,  $\gamma = 99.352(16)^\circ$ ,  $V = 2663.3(6)$  Å<sup>3</sup>,  $Z = 2$ ,  $\mu = 0.733$  mm<sup>-1</sup>, reflections collected/unique = 16046/5827,  $R1 = 0.0690$ ,  $wR2 = 0.1774$ , GOF = 0.951.

CCDC reference numbers 208492 and 208493.

See <http://www.rsc.org/suppdata/dt/b3/b304122k/> for crystallographic data in CIF or other electronic format.

## Computational details

DFT calculations were performed with the Gaussian 98 series of programs<sup>23</sup> using the non-local hybrid functional denoted as B3LYP.<sup>24</sup> The B3PW91 functional<sup>25</sup> was also used in one case (for model A' described in Table 3).

For ruthenium, the core electrons were represented by a relativistic small-core pseudopotential determined according to the Durand–Barthelat method.<sup>26</sup> The sixteen electrons corresponding to the 4s, 4p, 4d, and 5s atomic orbitals were described by a (7s, 6p, 6d) primitive set of Gaussian functions contracted to [5s, 5p, 3d]. Standard pseudopotentials developed in Toulouse were used to describe the atomic cores of carbon, oxygen, silicon and phosphorus.<sup>27</sup> A double-zeta plus polarization valence basis set was employed for each atom. d-Type polarization function was added for silicon and phosphorus (exponents 0.45). For hydrogen, a standard (4s) primitive basis contracted to [2s] was used. A p-type polarization function (exponent 0.90) was added for the hydrogen atoms directly bound to ruthenium. The geometries of the different species under consideration were optimized using analytic gradient. In the case of the model complex  $\text{Ru}_2\text{H}_2(\text{H}_2\text{Si}(\text{OMe})_2)_3(\text{PH}_3)_2$  a second optimization was also performed by adding a f-type polarization function (exponent 1.2) to the previous basis set (see C' in Table 3). The harmonic vibrational frequencies of the different stationary points of the PES have been calculated at the same level of theory in order to identify the local minima as

well as to estimate the corresponding zero-point vibrational energy (ZPE). Binding energies of the  $\text{SiH}_4$  ligand on the unsaturated fragment  $\text{RuH}_2(\text{PH}_3)_2$  were also calculated. The nature of the metal–silane interaction was analysed using natural bond orbital (NBO) calculations.<sup>28</sup>

## Acknowledgements

This work is supported by the CNRS. We thank the CINES (Montpellier, France) for a generous allocation of computer time.

## References

- (a) J. C. Lochart, *Chem. Rev.*, 1965, **65**, 131; (b) K. Moedritzer, *J. Organomet. Chem.*, 1966, **1**, 179 (*Adv. Organomet. Chem.*, 1966, **6**, 171); (c) V. Chvalovsky, *Organomet. React.*, 1972, **3**, 191; (d) M. D. Curtis and P. S. Epstein, *Adv. Organomet. Chem.*, 1981, **19**, 213; (e) L. G. Bell, W. A. Gustavson, S. Thanedar and M. D. Curtis, *Organometallics*, 1983, **2**, 740; (f) S. Xin, C. Aitken, J. F. Harrod, Y. Mu and E. Samuel, *Can. J. Chem.*, 1990, **68**, 471; (g) L. Hao, A. M. Lebus, J. F. Harrod and E. Samuel, *Chem. Commun.*, 1997, 2193; (h) L. Hao, A. M. Lebus and J. F. Harrod, *Chem. Commun.*, 1998, 1089; (i) D. C. Pestena, T. S. Koloski and D. H. Berry, *Organometallics*, 1994, **13**, 4173; (j) J. A. Reichl and D. H. Berry, *Adv. Organomet. Chem.*, 1999, **43**, 197; (k) M. Itoh, K. Inoue, J.-I. Ishikawa and K. Iwata, *J. Organomet. Chem.*, 2001, **629**, 1; (l) A. Purkayastha and J. B. Baruah, *Phosphorus, Sulfur, Silicon*, 2001, **169**, 9; (m) A. D. Sadow and T. D. Tilley, *Organometallics*, 2001, **20**, 4457.
- (a) X. L. Luo, G. J. Kubas, C. J. Burns, J. C. Bryan and C. J. Unkefer, *J. Am. Chem. Soc.*, 1995, **117**, 1159; (b) G. J. Kubas, *Metal dihydrogen and  $\sigma$ -bond complexes*, Kluwer Academic/Plenum Publishers, New York, 2001.
- K. Rahimian and J. F. Harrod, *Inorg. Chim. Acta*, 1998, **270**, 330.
- H.-G. Woo, R. H. Heyn and T. D. Tilley, *J. Am. Chem. Soc.*, 1992, **114**, 5698.
- I. Atheaux, B. Donnadiou, V. Rodriguez, S. Sabo-Etienne, B. Chaudret, K. Hussein and J.-C. Barthelat, *J. Am. Chem. Soc.*, 2000, **122**, 5664.
- (a) K. Hussein, C. J. Marsden, J.-C. Barthelat, V. Rodriguez, S. Conejero, S. Sabo-Etienne, B. Donnadiou and B. Chaudret, *Chem. Commun.*, 1999, 1315; (b) S. Sabo-Etienne, M. Hernandez, G. Chung, B. Chaudret and A. Castel, *New J. Chem.*, 1994, **18**, 175.
- I. Atheaux, F. Delpech, B. Donnadiou, S. Sabo-Etienne, B. Chaudret, K. Hussein, J.-C. Barthelat, T. Braun, S. B. Duckett and R. N. Perutz, *Organometallics*, 2002, **21**, 5347.
- J. Y. Corey and J. Braddock-Wilking, *Chem. Rev.*, 1999, **99**, 175.
- H. Ogino and H. Tobita, *Adv. Organomet. Chem.*, 1998, **42**, 223.
- F. Delpech, S. Sabo-Etienne, J.-C. Daran, B. Chaudret, K. Hussein, C. J. Marsden and J.-C. Barthelat, *J. Am. Chem. Soc.*, 1999, **121**, 6668.
- M. L. Christ, S. Sabo-Etienne and B. Chaudret, *Organometallics*, 1994, **13**, 3800.
- E. Gutierrez-Puebla, A. Monge, M. Paneque, M. L. Poveda, S. Taboada, M. Trujillo and E. Carmona, *J. Am. Chem. Soc.*, 1999, **121**, 346.
- T. Takao, S. Yoshida, H. Suzuki and M. Tanaka, *Organometallics*, 1995, **14**, 3855.
- Z. Lin, *Chem. Soc. Rev.*, 2002, **31**, 239.
- F. Maseras, A. Lledos, E. Clot and O. Eisenstein, *Chem. Rev.*, 2000, **100**, 601.
- K. Hussein, PhD thesis, Université Paul Sabatier, Toulouse, France, 2000.
- J. K. Hoyano, M. Elder and W. A. G. Graham, *J. Am. Chem. Soc.*, 1969, **91**, 4568.
- (a) S. Sabo-Etienne and B. Chaudret, *Coord. Chem. Rev.*, 1998, **178–180**, 381; (b) V. Rodriguez, S. Sabo-Etienne, B. Chaudret, J. Thoburn, S. Ulrich, H.-H. Limbach, J. Eckert, J.-C. Barthelat, K. Hussein and C. J. Marsden, *Inorg. Chem.*, 1998, **37**, 3475; (c) A. F. Borowski, B. Donnadiou, J.-C. Daran, S. Sabo-Etienne and B. Chaudret, *Chem. Commun.*, 2000, 543; A. F. Borowski, B. Donnadiou, J.-C. Daran, S. Sabo-Etienne and B. Chaudret, *Chem. Commun.*, 1967, 543.
- SIR92: A. Altomare, M. C. Burla, M. Camalli, G. Casciarano, C. Giacovazzo, A. Guagliardi and G. Polidori, *J. Appl. Crystallogr.*, 1994, **27**, 435.

- 
- 20 SHELX97 [Includes SHELXS97, SHELXL97, CIFTAB]- programs for Crystal Structure Analysis (Release 97-2) : G. M. Sheldrick, Institut für Anorganische Chemie der Universität, Tammanstrasse 4, D-3400 Göttingen, Germany, 1998.
- 21 WINGX L: J. Farrugia, *J. Appl. Crystallogr.*, 1999, **32**, 837.
- 22 ORTEP3 for Windows: L. J. Farrugia, *J. Appl. Crystallogr.*, 1997, **30**, 565.
- 23 M. J. Frisch, G. W. Trucks, H. B. Schlegel, G. E. Scuseria, M. A. Robb, J. R. Cheeseman, V. G. Zakrzewski, J. A. Montgomery, Jr., R. E. Stratmann, J. C. Burant, S. Dapprich, J. M. Millam, A. D. Daniels, K. N. Kudin, M. C. Strain, O. Farkas, J. Tomasi, V. Barone, M. Cossi, R. Cammi, B. Mennucci, C. Pomelli, C. Adamo, S. Clifford, J. Ochterski, G. A. Petersson, P. Y. Ayala, Q. Cui, K. Morokuma, P. Salvador, J. J. Dannenberg, D. K. Malick, A. D. Rabuck, K. Raghavachari, J. B. Foresman, J. Cioslowski, J. V. Ortiz, A. G. Baboul, B. B. Stefanov, G. Liu, A. Liashenko, P. Piskorz, I. Komaromi, R. Gomperts, R. L. Martin, D. J. Fox, T. Keith, M. A. Al-Laham, C. Y. Peng, A. Nanayakkara, M. Challacombe, P. M. W. Gill, B. G. Johnson, W. Chen, M. W. Wong, J. L. Andres, C. Gonzalez, M. Head-Gordon, E. S. Replogle and J. A. Pople, GAUSSIAN 98 (Revision A.11), Gaussian, Inc., Pittsburgh, PA, 2001.
- 24 (a) A. D. Becke, *J. Chem. Phys.*, 1993, **98**, 5648; (b) C. Lee, W. Yang and R. G. Parr, *Phys. Rev. B.*, 1988, **37**, 785.
- 25 J. P. Perdew and Y. Wang, *Phys. Rev. B.*, 1992, **45**, 13244.
- 26 P. Durand and J.-C. Barthelat, *Theor. Chim. Acta*, 1975, **38**, 283.
- 27 Y. Bouteiller, C. Mijoule, M. Nizam, J.-C. Barthelat, J.-P. Daudey, M. Pélissier and B. Silvi, *Mol. Phys.*, 1988, **65**, 2664.
- 28 A. E. Reed, L. A. Curtiss and F. Weinhold, *Chem. Rev.*, 1988, **88**, 899.